Assessment of Soil Erosion Using GIS Base Erosion Potential Method. Case Study of Victoria Reservoir Watershed

E.M.G.T.G.V.D.Premarathne [1#], I.A.K.S. Illeperuma [2]

[1]*Department of Remote Sensing and GIS, Faculty of Geomatics, Sabaragamuwa University of Sri Lanka, Sri Lanka*
[2]*Department of Remote Sensing and GIS, Faculty of Geomatics, Sabaragamuwa University of Sri Lanka, Sri Lanka*
[#] <vishvapremarathna@gmail.com>

Abstract— *Soil erosion is a serious environmental problem that adversely affects ecosystem health and land productivity. Effective land management and erosion control strategies depend on accurate assessment and identification of areas vulnerable to soil erosion. To identify areas prone to erosion, this study focuses on soil erosion assessment using a geographic information system (GIS)-based erosion potential method. The study used different layers of data including topography data, land cover, soil properties, rainfall and temperature patterns to estimate the overall erosion potential model. GIS technology facilitated the integration and analysis of these data layers, enabling a spatially clear assessment of erosion risk across the study area. The results of the erosion potential assessment revealed spatial patterns of erosion susceptibility across the study area. It ranges from 0.008 m3 m-2 year-1 to 3.2 m3 m-2 year-1. Areas with little vegetation and areas with steep slopes were found to have a higher potential for erosion. On the other hand, areas with abundant vegetation and gentle slopes showed less potential for erosion. The analysis highlighted the influence of rainfall and temperature, highlighting the importance of considering climatic factors in erosion assessment. The findings of this research provide valuable insights for land managers and policymakers in implementing targeted soil conservation measures.*

Keywords— **soil erosion, erosion potential method, GIS, Victoria reservoir watershed**

I. INTRODUCTION

One type of soil degradation is known as soil erosion, which is the displacement of the top layer of soil. Soil erosion is one of the most prevalent form of land degradation worldwide, causing significant environmental and socio-economic problems. Land attributes such as soil depth and crop-growing capability in steep terrain, soil fertility, crop yields, and quality, floral biodiversity, groundwater retention for home gardens, waterfall beauty, and surface water quality are all negatively impacted by soil erosion processes.

The color of many rivers and streams turns brown during the rainy season, indicating off-site soil erosion. This effect strips away the fertile topsoil, rendering it unsuitable for agriculture. Also, they pose a threat to water quality and the survival of aquatic life by depositing in reservoirs. Therefore, soil erosion reduction techniques should be implemented.

Globally, many researchers have developed various soil loss assessment models, however, each model has its inherent limits based on input availability, scope of application, and associated level of complexity (Behera *et al.*, 2020). Soil erosion can be calculated using field data or Remote Sensing and GIS base models. Several models are used to assess soil erosion, classified as empirical or regression models, conceptual models, and physics-based models. Additionally, they can be classified as qualitative, quantitative, and semi-quantitative models (Dragičević, Karleuša and Ožanić, 2016). However, due to the large amount of data needed and the modeler's lack of experience among modelers, most worldwide applications are restricted to the use of empirical models (Behera *et al.*, 2020). The most common empirical models for estimating soil erosion include the Revised Universal Soil Loss Equation (RUSLE) method, the Erosion Potential Method (EPM), the Water Erosion Prediction Project (WEPP) method, the Universal Soil Loss Equation (USLE), and the Pacific Southwest Interagency Committee (PSIAC) method.

Slobodan Gavrilovi created the Gavrilovi model, also known as the Erosion Potential Model (EPM), based on field studies he conducted on erosion in the Morava River watershed area in Serbia in the 1960s. This method itself is based on the Method for the Quantitative Classification of Erosion (MQCE), formally developed in 1954 (Ahmed *et al.*, 2019). The EPM combines water erosion factors based on precipitation, temperature, soil erodibility, soil protection, types of erosion, and slopes. A quantitative map of water erosion in m^3 m^{-2} $year^{-1}$ was created by superimposing the numerous components mentioned above on a platform of geographic information systems. A classified map according to the amount of soil erosion was prepared using EPM.

II. METHODOLOGY AND EXPERIMENTAL DESIGN

A. Study Area

The Victoria Reservoir Watershed was selected as a study area for assessment of soil erosion. It is located in the central province of Sri Lanka. There are significant topographical changes throughout the mountainous watershed. The extent of watershed is around 1330 square kilometers. The elevation is between 407 and 2,130 meters above mean sea level and 800 meters being average. The mean average annual precipitation and the mean temperature of the study area are 2006.6 mm and 24.6 ^{0}C

respectively. Many agricultural lands, reserves, rural areas, and urban areas are included in the study area.

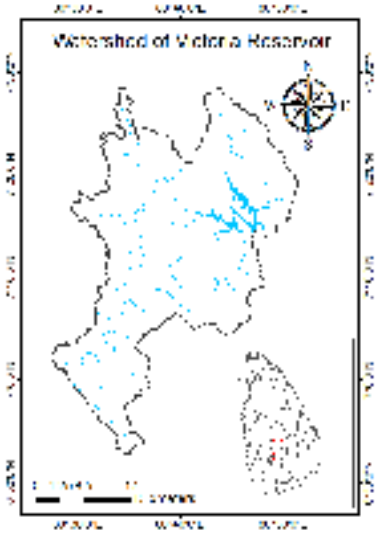

Figure 1 Map of the study area

B. Materials

Table 1. Description of Data

Data	Source	EPM factor
Landsat 8 satellite images from 2014 to 2020	USGS Earth Explorer	Temperature coefficient, Soil protection coefficient, Existing erosion coefficient
Soil data	3D soil database in Sri Lanka	Soil erodibility coefficient
Precipitation data	Meteorology department	Average annual precipitation
Digital Elevation Model	USGS Earth Explorer	Slope index

C. Methodology

Figure 2. Flow chart of the methodology

1) Temperature Coefficient

The Temperature Coefficient was calculated using equations (1) to (7), band 10, and metadata file provided with Landsat 8 images.

Spectral radiance-L($W.m^{-2}.sr^{-1}.\mu m^{-1}$)

$$L = M_L Q_{cal} + A_L \quad (1)$$

Where:

M_L-Band specific multiplicative rescaling factor from metadata

Q_{cal}-Quantized and calibrated standard product pixel value in Digital Number (DN)

A_L-Band specific additive rescaling factor from metadata

Brightness temperature-BT

$$BT = \frac{K_2}{\ln\left(\frac{K_1}{L} + 1\right)} - 273.15 \quad (2)$$

Where:

K_1, K_2-Calibration constants

The Normalized Difference Vegetation Index-$NDVI$

$$NDVI = \frac{band\ 5 - band\ 4}{band\ 5 + band\ 4} \quad (3)$$

The proportion of vegetation-P_v

$$P_v = \sqrt{\frac{NDVI - NDVI_{min}}{NDVI_{max} - NDVI_{min}}} \quad (4)$$

Emissivity ε

$$\varepsilon = 0.004 \times P_v + 0.986 \quad (5)$$

Land Surface Temperature-LST

$$LST = \frac{BT}{1 + \frac{0.00115 \times BT}{1.4388} \times \ln \varepsilon} \quad (6)$$

(franpc, 2019)

Repeated this step for three years: 2014, 2017, and 2020 and Got average annual temperature-T_0

Temperature Coefficient-T

$$T = \sqrt{\left(\frac{T_0}{10}\right)} + 0.1 \quad (7)$$

2) Average Annual Precipitation

An average annual precipitation map (P) was produced using rainfall station data. Annual precipitation was calculated using monthly rainfall station data for each rainfall station from each year and the average annual precipitation of each rainfall station. Kriging interpolation was used to prepared an average annual precipitation map.

3) Soil Protection Coefficient

XaNDVI, a modified version of the NDVI, was used to estimate the soil protection coefficient. The Soil Protection Coefficient was calculated with equations (8) and (9) using bands 4 and 7 of Landsat 8 images.

Modified NDVI- X_aNDVI

$$X_a NDVI = \frac{band\ 4 - band\ 7}{band\ 4 + band\ 7} \quad (8)$$

(Jurgens, 1997)

Soil Protection Coefficient- X_a

$$X_a = (X_a NDVI - 0.9363)(-0.7769) \quad (9)$$

(Chaaouan *et al.*, 2013)

4) Soil Erodibility Coefficient

There are several methods to calculate the soil erodability coefficient. In this study it was calculated by using a model developed by Williams, Jones, and Dyke (Sharpley and Williams, 1990) with equation (10) and equation (11). Soil Erodibility Coefficient(Y) was calculated using sand, clay, silt percentage, and organic carbon content of soil.

$$SN1 = 1 - \frac{SAN}{100} \quad (10)$$

$$Y = \left\{0.2 + 0.3 \exp\left[0.0256 SAN \left(1 - \frac{SIL}{100}\right)\right]\right\} \left(\frac{SIL}{CLA+SIL}\right)^{0.3} \left[1.0 - \frac{0.25C}{C+\exp(3.72-2.95C)}\right] \left[1.0 - \frac{0.7SNI}{SNI+\exp(-5.51+2.95SN1)}\right] \quad (11)$$

Where:

SAN, SIL, and CLA are Sand, Silt, and Clay percentages

C-Organic carbon content

5) Existing Erosion Coefficient

The Existing Erosion Coefficient(φ) was calculated using equation (12).

$$\varphi = \sqrt{\left(\frac{TM4}{Q_{max}}\right)} \quad (12)$$

Where:
TM4- Band 4 of Landsat image 8
Q_{max}-Maximum value of the radiance
(El Badaoui *et al.*, 2021)

6) Slope Index

A Slope map was created using DEM and classified to get Slope Index(Ja).

7) Erosion Intensity Coefficient

The Erosion Intensity Coefficient(Z) was calculated using equation (13).

$$Z = X_a Y(\varphi + \sqrt{J_a}) \quad (13)$$

8) Average Annual Soil Erosion

Finally, Average Annual Soil Erosion(W) was estimated with equation (14).

$$W = TP\pi\sqrt{Z^3 F} \quad (14)$$

Where:
F- Watershed surface area

(Zeghmar, Marouf and Mokhtari, 2022)

III. RESULTS

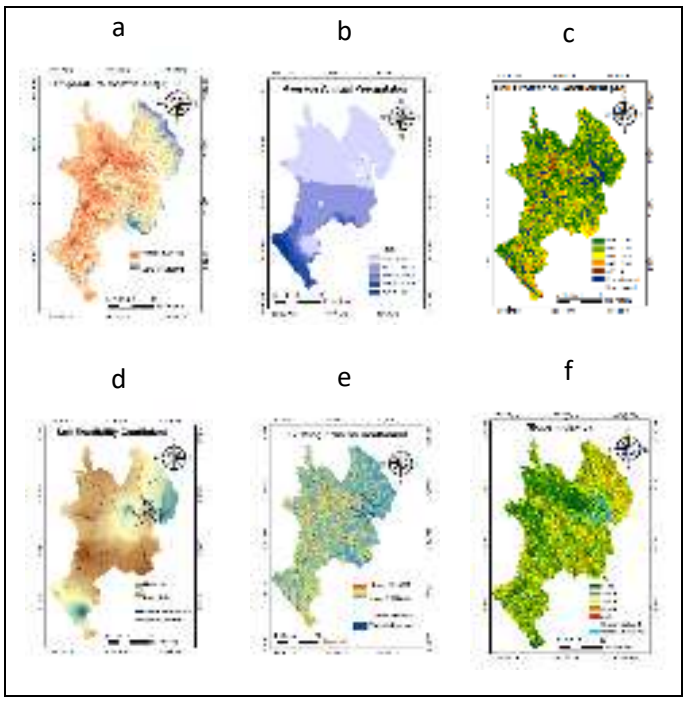

Figure 3. Factor maps of the study area

A. Temperature Coefficient

In mechanical weathering activities, temperature is a crucial indicator. since these affect the moisture of rocks and sediments, which causes the oxidation, hydration, and breakdown of rock minerals (Zeghmar, Marouf, and Mokhtari, 2022).

B. Average Annual Precipitation

In the context of soil erosion, precipitation plays a vital role as a driving factor for water-related erosion processes. It was worth noting that the average annual soil erosion in the study area ranges from 1247 mm to 4637 mm. (Figure 3-b)

C. Soil Protection Coefficient

The soil protection coefficient varies with the vegetation cover of the study area. Vegetation cover increases the roughness of the soil surface and prevents water from flowing over the soil surface and prolongs infiltration time. The soil protection coefficient value ranges from 0.05 for areas with dense vegetation to 1.0 for bare soils (Sakuno *et al.*, 2020). Generated soil protection coefficient map is shown in Figure 3 (c).

Table 2 Area representation of Xa classes

Value Range	Area (Km^2)
0.05-0.26	401.69
0.26-0.34	438.01
0.34-0.43	293.83
0.43-0.55	132.63
0.55-1.00	41.41

Table 2 gives the area extent of the different levels of the soil protection coefficient Table indicates that most of the study area has a soil protection coefficient of less than 0.4.

D. Soil Erodibility Coefficient

Figure 3 (d) shows the generated soil erodibility coefficient map of the study area and its ranges from 0.18 to 0.49. This map indicates how easily soil particles can get detached and be carried away by runoff and precipitation. So high values of the map indicate, a high inherent erodibility area.

E. Existing Erosion Coefficient

Erosion processes in the watershed are assessed and ranked based on the current erosion coefficient, which determines the areas that are eroded and has a value between 0.1 and 1.0. Figure 3 (e) shows the existing erosion coefficient map of the study area and it has a value ranging from 0.29 to 0.70. This indicates that the area is eroded and according to the map, most of the areas are less eroded. Also, considerable amount of area extent shows moderately eroded.

F. Slope Index

The slope index extracted by SRTM DEM. Table 3 gives the area extent of different classes within the study area.

Table 3 Area representation of slope index classes

Slope Percentage (%)	**Area (Km^2)**
0-10	360.55
10-20	552.83
20-30	297.51
30-40	77.80
40<	16.62

G. Erosion Intensity Coefficient

The erosion intensity coefficient tracks the severity of erosion in the watershed and provides information on erosion's likelihood and intensity while not providing information about the expected sediment production (Dragičević, Karleuša and Ožanić, 2016). Obtained results are classified into 5 levels and shown in Figure 4.

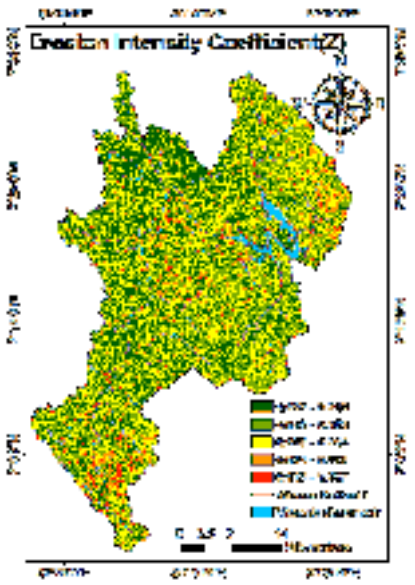

Figure 4. Erosion intensity coefficient map of the study area

Table 4 Area representation of erosion intensity classes

Erosion Intensity(Z) Range	**Area (Km^2)**	**Classified Intensity Levels**
0.007<Z<0.046	372.54	Very low intensity
0.046<Z<0.063	454.11	Low intensity
0.063<Z<0.084	302.66	Moderate intensity
0.084<Z<0.113	138.31	High intensity
0.113<Z<0.257	36.20	Very high intensity

A significant amount of the study area has an Erosion Intensity between 0.046 and 0.63, it is numerically 454.11 km2(35% of the study area).

H. Average Annual Soil Erosion

Figure 5 shows the Average Annual Soil Erosion map. The map shows the amount of soil being eroded in cubic meters per square meter per year.

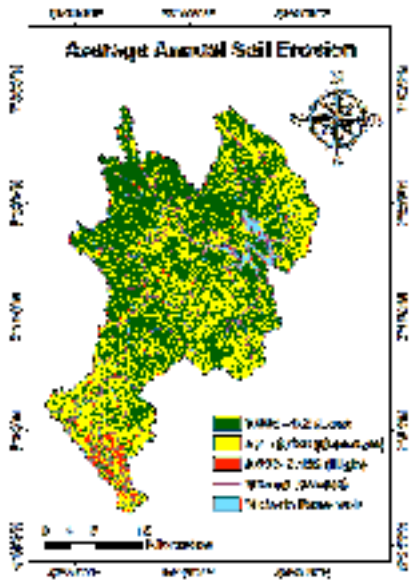

Figure 5. Average annual soil erosion map of the study area

The amount of soil loss was calculated using Erosion Intensity Coefficient with climate factors such as Rainfall and Temperature. The soil losses were divided into three categories such as low, moderate, and high, and calculated soil loss was tabulated in table 5.

Table 5 Area of soil losses

Range of Average Annual Soil Losses ($m^3m^{-2}year^{-1}$)	**Area(Km^2)**	**Percentage of Total Area**
0.008-0.200 (Low)	902.47	69.30%
0.200-0.596 (Moderate)	358.69	27.53%
0.596-3.198 (High)	41.318	3.17%

III. DISCUSSION AND CONCLUSION

A. Discussion

The model outputs are mainly derived from the multiplication of its parameters. Therefore, there is a direct relationship between the model coefficients and the Erosion Intensity Coefficient. Based on a visual comparison of the results, it appears that there is a stronger correlation between the Erosion Intensity Coefficient and Soil Protection Coefficient. Table 6 gives a percent of the area covered by the highest values of soil intensity intersect with the area of the highest values of considering coefficient. According to table 5 61.23% of the area covered by the highest values of erosion intensity intersect with the area of the highest values of soil protection coefficient. The above percentages of the Slope index, Existing Erosion Coefficient and Soil Erodability Coefficient are 14.37%, 8.37%, and 3.27% respectively.

Table 6 Area comparison between erosion intensity and its related factors

Factor	**Area with Highest Values(Km^2)**	**Percentage of the area covered by the highest values of erosion intensity intersects with the area of the highest values of considering coefficients**
Soil Protection Coefficient	106.85	61.23%
Slope Index	25.07	14.37%
Existing Erosion Coefficient	14.60	8.37%
Soil Erodability Coefficient	5.70	3.27%

Applying the EPM model resulted in the greatest amounts of soil loss on the South side of the study area, ranging from 0.5 $m^3m^{-2}year^{-1}$ to 3.2 $m^3m^{-2}year^{-1}$. The highest amount of soil erosion was observed in the Nuwara Eliya District which experiences high rainfall throughout the year. When comparing climate factors, Rainfall is a crucial factor for soil erosion case of water. 58.5 % of the area covered by the highest values of Average Annual Soil losses intersect with the area of the highest values of Average Annual Precipitation.

Table 7 Area comparison between soil losses and its related factors

Factor	**Area with Highest Values(Km^2)**	**Percent of the area covered by the highest values of average annual soil erosion overlay with the area of the highest values of considering factors**
Rainfall	24.18	58.54%
Temperature	16.77	40.60%
Erosion Intensity Coefficient	39.46	95.52%

According to table 7, 95.52% of the area covered by the highest values of Average Annual Soil losses overlay with the area of the highest values of Erosion Intensity coefficient. Considering all factors, around 3% of the study area has high soil losses due to mainly rainfall, vegetation covers, and slope.

B. Conclusion

The results of this study emphasize the importance of patterns in land cover, topography, rainfall, temperature, and soil properties in determining erosion potential. These elements are successfully incorporated into the GIS-based erosion potential method to provide an evaluation of erosion risk throughout the study area. Areas with a high potential for erosion can be identified by precise mapping and analysing the terrain using GIS tools, allowing the implementation of focused soil conservation measures

From the analysis, it can be concluded that the soil protection coefficient has a very high effect on soil erosion intensity while the slope index shows a moderate effect. But existing erosion coefficient and soil erodability coefficient have less effect on soil erosion intensity.

From analysis, it can be concluded that high rainfall, temperature coefficient, and slope index area get high soil loss. In other words, high soil erosion can be observed within those areas.

REFERENCES

Ahmed, A. *et al.* (2019) 'Using EPM Model and GIS for Estimation of Soil Erosion in Souss Basin, Morocco', *Turkish Journal of Agriculture - Food Science and Technology*, 7(8), pp. 1228–1232. Available at: https://doi.org/10.24925/turjaf.v7i8.1228-1232.2562.

El Badaoui, K. *et al.* (2021) 'Erosion Potential Method (Gavrilović Method): Methodological improvements and application in Toudgha River catchment, southeast of Morocco', *International Journal Water Sciences and Environment Technologies V*, 6(1), pp. 114–123. Available at: www.jiste.org.

Behera, M. *et al.* (2020) 'Integrated GIS-based RUSLE approach for quantification of potential soil erosion under future climate change scenarios', *Environmental Monitoring and Assessment*, 192(11). Available at: https://doi.org/10.1007/s10661-020-08688-2.

Chaaouan, J. *et al.* (2013) 'Télédétection, sig et modélisation de l'érosion hydrique dans le bassin versant de l'oued amaz, Rif Central', *Revue Francaise de Photogrammetrie et de Teledetection*, (203), pp. 19–25. Available at: https://doi.org/10.52638/rfpt.2013.26.

Dragičević, N., Karleuša, B. and Ožanić, N. (2016) 'A review of the Gavrilovićameruamam method (erosion potential method) application', *Gradjevinar*. Union of Croatian Civil Engineers and Technicians, pp. 715–725. Available at: https://doi.org/10.14256/JCE.1602.2016.

francpc (2019) 'How to calculate Land Surface Temperature with Landsat 8 satellite imagesTitle', *GeoGeek*, (L), pp. 1–5. Available at: https://giscrack.com/how-to-calculate-land-surface-temperature-with-landsat-8-images/ (Accessed: 11 May 2023).

Jurgens, C. (1997) 'The modified normalized difference vegetation index (mNDVI) a new index to determine frost damages in agriculture based on landsat TM data', *International Journal of Remote Sensing*, 18(17), pp. 3583–3594. Available at: https://doi.org/10.1080/014311697216810.

Sakuno, N.R.R. *et al.* (2020) 'Adaptation and application of the erosion potential method for tropical soils', *Revista Ciencia Agronomica*, 51(1), pp. 1–10. Available at: https://doi.org/10.5935/1806-6690.20200004.

Sharpley, A.N. and Williams, J.R. (1990) 'EPIC: The erosion-productivity impact calculator', *U.S. Department of Agriculture Technical Bulletin*, (1768), p. 235. Available at: http://agris.fao.org/agris-search/search.do?recordID=US9403696.

Zeghmar, A., Marouf, N. and Mokhtari, E. (2022) 'Assessment of soil erosion using the GIS-based erosion potential method in the Kebir Rhumel Watershed, Northeast Algeria', *Journal of Water and Land Development*, 52, pp. 133–144. Available at: https://doi.org/10.24425/jwld.2022.140383.

ACKNOWLEDGMENT

I would like to extend my heartfelt appreciation to the Research Unit of the Faculty of Geomatics, Sabaragamuwa University of Sri Lanka, for their unwavering support during my research. Their valuable guidance and assistance have played a crucial role in the successful completion of this abstract.

AUTHOR BIOGRAPHIES

I.A.K.S. Illeperuma, Senior Lecturer at the Department of Remote Sensing and GIS, Sabaragamuwa University of Sri Lanka. She is mainly teaching GIS, Satellite Technology, and Digital Elevation Modelling and conducting relevant practicals for undergraduate students in the faculty. She has qualifications such as M.Sc. Remote Sensing and Geographical Information System, School of Engineering and Technology, Asian Institute of Technology, Thailand. 2008, Post Graduate Diploma(GIS Remote Sensing & Photogrammetry) Wuhan Technical University of Surveying and Mapping, China. 1999, BSc (Surveying Sciences), Institute of Surveying and Mapping, Sri Lanka. 1997.

E.M.G.T.G.V.D. Premarathne, an undergraduate student following BSc(Hons.) Surveying Sciences degree in the Department of Remote Sensing and GIS, Sabaragamuwa University of Sri Lanka.